Impact of the air-side and methane-side dilution (CO_2, N_2, Ar) on the lifting process of a non-premixed jet-flame

M. Marin [*, 1], F. Baillot [1], G. Godard[1]
[1]Laboratory CORIA – UMR 6614, CNRS-Université et INSA de Rouen, France.

Abstract
In the non-premixed regime mixing of reactants is a key element in several basic phenomena among which flame stabilization and pollutant formation are noted. This work aims to investigate the response of a non-premixed flame when the **air-side** or the **methane-side** is diluted by a chemically weak or inert diluent (CO_2, N_2, Ar). The first mechanisms due to aerodynamics or dilution are recognized and the dimensionless numbers piloting the flame lifting process are identified. For that purpose several quantities are measured: the critical ratios at lifting, $(Q_d/Q_{ox})_{lift}$ and $(Q_d/Q_f)_{lift}$, where Q_d, Q_f and Q_{ox} are the volumetric flows rates of the diluent, fuel and oxidant respectively; the attachment flame height H_a and radius R_a. Results show that the flame lifting process is controlled at the main order by the propagation flame-leading-edge approach at the flame base.

1. Introduction

Dilution is a crucial topic which plays an important role in exhaust gas recirculation combustion systems to improve combustion efficiency and diminish pollutants emissions. As shown in [1,2,3], when the air is diluted by an inert or chemically weak diluent four main impacts involved in non-premixed jet-flame stability have been identified: i) pure dilution effect, ii) thermal action effect, iii) transport properties effect and iv) chemical effect. This work pursues the previous study concerning the transition from an attached flame to a lifted flame when the air was diluted, but now, by diluting either the air or the methane streams and by comparing results of the two configurations**.** For this purpose, the three diluents: CO_2, N_2, and Ar have also been used. It helps to discriminate between the main abovementioned mechanisms which participate in the attachment flame stability as shown by [1]. A large range of methane velocities U_{CH4} reveals the competition between dilution and initial CH_4 jet aerodynamics on flame lifting. In particular, basic differences are noted according to the way dilution is performed, either in the air-side or in the methane-side. Adding a species in the methane or in the air leads to increase the flow rates velocities of the fuel $U_f = U_{CH4} + U_d$ (index "f" means "CH_4 + diluents") or of the oxidant $U_{ox} = U_{air} + U_d$ (ox=air + diluent). It induces a mechanical impact susceptible to help to break flame stability by this induced aerodynamics. Indeed, if that mechanical impact participates in such a stability loss by diluting the methane, it remains negligible with the air dilution. This work focuses on identifying the first mechanisms and dimensionless numbers which describe the flame liftoff as the air or methane is diluted. The analysis is carried out by introducing critical ratios at lifting, $(Q_d/Q_{ox})_{lift}$ and $(Q_d/Q_f)_{lift}$,. They evaluate the sensitivity of dilution impact according to the side dilution. Results show $(Q_d/Q_f)_{lift}/(Q_d/Q_{ox})_{lift}$ varies between ~ 3-6 depending on diluent properties. This feature is interpreted via a flame-leading-edge approach for which reactants are mixed around stoichiometric proportions in the flame base vicinity. It shows that leading-edge drives lifting phenomenon at the main order.
When dilution increases, the leading-edge of the attached flame moves nearby the burner rim and can be stabilized in locations a priori dependent on both mechanical and dilution impacts. CH*-emission is collected to examine the leading-edge location. It is characterized by the flame radius R_a, controlled at the main order by the jet impulsion and the flame height H_a, controlled at the main order by dilution. Flame stability characterized by the attachment flame parameters: $(Q_d/Q_f)_{lift}$, $(Q_d/Q_{ox})_{lift}$, H_a, R_a, can be studied by means of the three diluents. Then, self-similarity laws are deduced by comparing results obtained with them, which highlights the self-similarity quantities piloting lifting.

2. Experimental configuration and the flame attachment domain

2.1 Experimental configuration

The experimental set-up is the same as that detailed in [1]. It is constituted of a confined atmospheric vertical square furnace 0.25 x 0.25 m^2 in which a methane jet and an air co-flow are injected. Each of the reactants (methane and air) can be mixed with a diluent (CO_2, N_2 or Ar) in an upstream blend chamber. The fuel (CH_4 + diluent) then passes through a round tube with an inner diameter D_i= 5.7 mm and a burner rim e_l=2.25 mm located in the middle of the furnace. Several quartz windows are installed in two opposite sides of the chamber in order to observe the flame and qualify quantities of the system by means of optical diagnostics. Air and methane flow-rate velocities are given in the ranges: $0.1 < U_{air} < 0.4$ m/s, $1 < U_{CH4} < 15$ m/s respectively

* Corresponding author: y.marin@coria.fr

leading to the methane Reynolds numbers: 400 < Re_{CH4} <5500. Gas flows are measured by mass flow meters "Hastings" with an accuracy of 1% full scale. Measurements of flame lifting limits defined hereafter are repeated at least three times.

Two optical techniques were used to investigate the flame structure: CH* chemiluminescence imaging and planar OH laser induced fluorescence (OH-PLIF). CH* imaging is carried out with a ICCD camera Princeton PI-max (10 fps, 512 X 512 pixels, 16-bits, exposure time: 3ms, resolution: 0.028 mm/pixel) and a 105 mm UV f/4.5 Nikon lens equipped with a band-pass filter BG12, centered at 400 nm with a 50 nm FWHM. Abel inversion has been applied to the instantaneous flame image to provide accurate planar information coming from the reaction zone in the flame base vicinity.

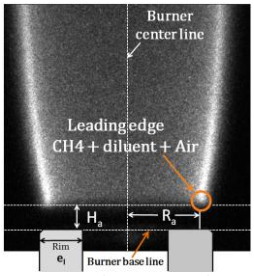

Figure 1. R_a and H_a at the flame base (flame-leading-edge)

The flame base position is defined as the lowest point where the maximum of the luminous CH* signal attains 2 times the background noise. Instantaneous attachment height $\tilde{H}_a$ ($\tilde{H}_a^o$ without dilution) is measured as the vertical distance between this point and the burner exit cross-section. The instantaneous attachment radius $\tilde{R}_a$ ($\tilde{R}_a^o$ without dilution) is measured as the horizontal distance between the point and the burner axis (see Fig. 1). Mean quantities H_a (H_a^o) and R_a (R_a^o) have been calculated by time-averaging 300 instantaneous data respectively. The emission of radical OH was collected by a ICCD - camera PIMAX4 (1024x1024 pixels, 10 fps) equipped with filters UG11 and WV305. For OH-PLIF the Q1(5) line of the (0, 1) vibrational band of (X2Π – A2Σ) was excited at λ~282.7 nm with a vertical laser sheet with 500 µm thick and 50 mm long.

2.2 Flame stability without dilution

2.2.1 The flame attachment domain

Lifting process occurs by increasing gas velocities. This usual procedure is used to define a stability domain which serves as a reference for the results obtained with dilution (see vertical arrows in fig. 2). For a given U_{air}, as U_{CH4} is increased the attached flame domain is observed until the flame lifts off. This upper limit specified by square dot line in fig. 2, defines the lifting velocity U_l. From this point, as U_{CH4} is decreased, reattachment is obtained for a lower limit U_a, namely the natural reattachment velocity. Boundaries $U_{CH4} = U_a$ and $U_{CH4} = U_l$ delimits the hysteresis domain where a flame may be attached or lifted for the same flow velocities. U_{air} does not affect U_a and U_l in the range 0.1 < U_{air} < 0.27 m/s, the fuel jet behaving as a free jet. For U_{air} > 0.27, U_l slightly decreases as U_{air} increases as shown in fig. 2. However, it remains very small and leads to conclude that flame stability is little affected by increasing U_{air} within the air range studied here. This feature relies on the semi-thick burner rim e_l behind which the flame stabilizes thanks to a slower flow, as explained in sec. 2.2.2. Indeed the rim influence was previously revealed in an experiment without dilution carried out by Wyzgolik and Baillot [4] but in the case of a thin rim (e_l ~ 0.2 mm). There, on the contrary to the present result, the hysteresis domain was strictly dependent on both U_{air} and U_{CH4} at lifting. It was described by the relationship: $U_l = -31.94U_{air} + 25.89$ where U_{air} evolved in the range 0 <U_{air} <0.63 m/s.

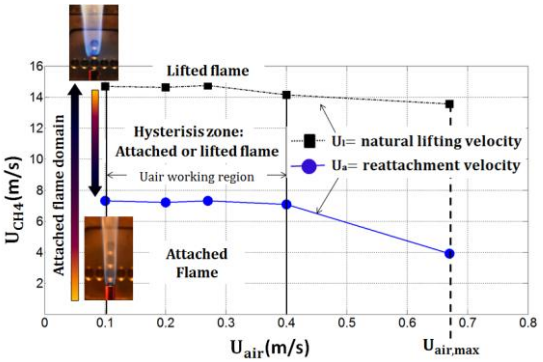

Figure 2. Hysteresis zone without dilution

For $U_{CH4} \leq U_l$, increasing U_{air} cannot lead to the flame lift off in this work, even for the maximum air co-flow velocity $U_{air,max}$=0.67 m/s, a limitation inherent to the experimental setup.

2.2.2 The flame base location $H_a°$ and $R_a°$

Varying U_{CH4} moves the flame base to a new location, characterized by H_a^o and R_a^o where the flame remains anchored in the near field of the burner rim. This location appears as a crucial quantity representative of the lifting process. Fig. 3 shows how H_a^o and R_a^o are modified when U_{CH4} is increased from U_{CH4}=1.1 m/s, up to $U_{CH4\text{-}lift} = U_l$ for the two air conditions U_{air} =0.1 and 0.4 m/s. By increasing U_{CH4} the flame is pushed towards the fuel stream with a slight increase in $H_a°$: H_a^o increases by a maximum variation ΔH_a^o ~ 0.32 mm at U_{air}=0.1 m/s and ~ 0.28 mm at U_{air}=0.4 m/s, while R_a^o decreases by a four times higher amount than that for H_a^o, with a maximum variation $|\Delta R_a^o|$ ~1.17 mm at U_{air}=0.1 and ~1 mm at U_{air}=0.4 m/s. Thus, the fuel jet aerodynamics more strongly impacts Ra^o than H_a^o. Finally the flame stabilizes radially closer to the fuel and axially slightly farther downstream.

This lateral flame displacement is directly linked to e_l. In the literature significant aerodynamic alterations were already observed in the flame stability by systematically changing e_l. For example, Y. Otakayema et al. [6] studied the influence of e_l on the stabilization mechanism of non-premixed air/methane jet flames issuing from rectangular slits of width s. For a thin burner rim ($e_l \leq 2.0$ mm), the flame gradually moved upward following a

vertical path by increasing U_f as was shown by [4, 5] before then; flame extinction or **blow-out** occurred at a large standoff distance from the burner (~ 6 s) via a lifted flame**.** For a thick rim ($e_l \geq 3.0$mm), the flame remained attached as U_f increased, by adapting its base location which laterally moved along the rim; extinction or **blow-off** suddenly occurred at a small distance (H_a°~ 0.3 s) without passing via a lifted state. Finally for a semi-thick rim ($2.0 < e_l < 3.0$ mm), the flame stability resulted from a compromise between the two effects explained above. Blow-out and blow-off were observed when the flame reached a critical $U_{f\text{-}lift}$ value which depended on the co-flow conditions.

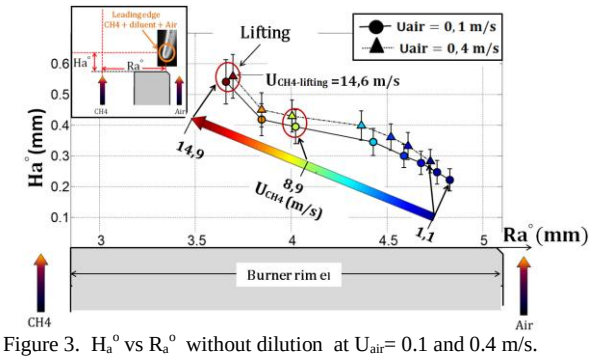

Figure 3. H_a^o vs R_a^o without dilution at U_{air}= 0.1 and 0.4 m/s.

Here e_l = 2.25 mm, an intermediate rim thickness, stabilizes the flame at its rear by diminishing $|\Delta R_a^o| \sim 0.5e_l$ jointly with a small increase in $\Delta H_a^o \sim 0.1e_l$. It agrees with the results of Juniper and Candel [5] who carried out a numerical simulation of hydrogen flame stability above a condensed oxygen surface behind a step. In that paper they examined the influence of the Damköler number Da and of the step height, which played the role of a rim thickness. If the flame thickness "δ_{fl}" was thinner than the step "e_l" the flame tucked behind it within a slow flow region. The flame was then very little affected by Da variation. By contrast, if the flame thickness was wider than the step, the flame was forced out and the standoff distance increased; the flame was very sensitive to Da variation.

In our work, flame thicknesses without dilution, based on the maximum LIF-OH and CH* intensity gradients, were measured in the flame base vicinity. $\delta_{fl\text{-}CH^*}=0.1e_l$ and $\delta_{fl\text{-}OH}=0.33e_l$ are smaller than e_l, which explains the abovementioned lateral flame displacement.

3. Air-side and methane side dilutions

3.1 Mechanical impact of dilution.

Fuel velocity U_f and oxidant velocity U_{ox} increase as a diluent is added to the initial methane or air stream respectively. The velocity augmentation can participate in lifting the flame off by a pure aerodynamic effect as explained in 2.2. But it also depends on the diluent capacity to destabilize the flame: the more efficient the diluent to break the attached flame stability, the less the diluent amount is needed and the smaller the induced mechanical impact. Thus adding CO2, N2 and Ar into the air (methane) increases the stream velocity at the most by 10 – 30% of U_{air} (200 – 300% of U_{CH4}) the data corresponding to the maximum diluent amount measured at lifting for U_{CH4}=1.1 m/s.

To appreciate this impact for each side dilution, the oxidant and fuel velocities at lifting must be compared to the natural lifting velocities: $U_{air,lift}$ and U_l=$U_{CH4,lift}$ respectively. However, as mentioned in 2.2.1. $U_{air,lift}$ cannot be attained with the set-up. So, to ensure the comparison, the maximum accessible air velocity, $U_{air,max}$ = 0.67 m/s is used here. We introduce the parameters $\Delta U_{ox,lift} / U_{air,max} = (U_{ox} - U_{air})_{lift} / U_{air,max}$ and $\Delta U_{f,lift} / U_l = (U_f - U_{CH4})_{lift} / U_l$ which are plotted in fig. 4 as functions of U_{CH4} for U_{air}=0.1 m/s. In both dilution configurations the change in the initial methane jet from laminar to turbulent is remarkable on these parameters.

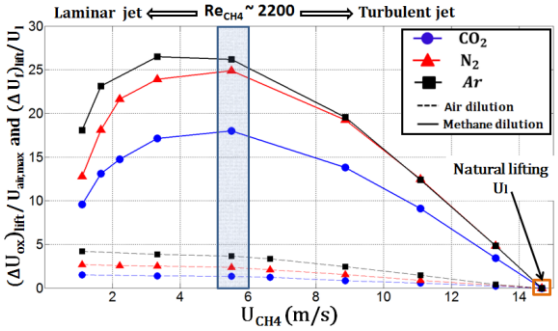

Figure 4. $\Delta U_{ox,lift}/U_{air,lift}$ and $\Delta U_{f,lift}/U_l$ against U_{CH4} at U_{air}=0.1 m/s

In the **air-dilution** case (see fig. 4) a change in the slope is noted when the initial methane jet regime becomes turbulent (Re_{CH4}~2200). $\Delta U_{ox,lift}/U_{air,max}$ ranges between 2 – 5 %. It completes the results of Min et al. [1] who in a similar configuration carried out experimental procedures with the same diluents (CO_2, N_2, Ar) at U_{air}=0.1 m/s in order to quantify the mechanical impacts on the flame attachment height at lifting $H_{a,lift}$. They found that $H_{a,lift}$ differed by no more than 5%, despite the velocity augmentations. All these features highlight flame stability presents a small sensitivity to the air co-flow velocity augmentation within the domain investigated here. It is also consistent with the flame behavior noted without dilution, since its base location, specified by (R_a°, H_a°), presents very small variations when U_{air} varies from 0.1 to 0.4 m/s whatever U_{CH4} (see fig. 3). To conclude, mechanical impacts are negligible in the air dilution.

In the **methane-side** dilution, the stream velocity increases more than in the air-side dilution. Results in fig. 4 show that whatever the diluents $\Delta U_{f,lift} / U_l$ evolves as a bell–shape. The maximum attains 18% with CO2, 25% with N2 and 27 % with Ar where the regime of the pure CH_4 jet changes from laminar to turbulent (Re_{CH4} ~ 2200). The mechanical impact cannot be assumed negligible. Thus, it participates in the behavior differences noted between the air-side and methane-side dilutions as shown hereafter. However, the diluent nature does play the key role in the flame lifting process.

3.2 Competition between aerodynamics and dilution impacts

Under given initial non-diluted aerodynamic conditions (U_{CH4}, U_{air}), dilution with CO_2, N_2 and Ar, affects flame stability according to the diluent properties [1, 2, 7]. N_2

which has thermal and transport properties similar to the air, influences stability via only a pure dilution effect. **CO_2** addition causes flame lift-off by pure dilution, but also by thermal and chemical actions; pure dilution is the most significant effect, followed by the thermal effect and finally by the chemical effect which is, however, small. The three effects diminish flame stability and lead to lift off the flame. As with the two previous diluents, **Ar** addition leads to a main pure dilution effect able to break flame stability. Nevertheless, it is countered by thermal and transport properties. As seen, these various actions depending on the diluent nature combine with the mechanical impact, as soon as it is not negligible to participate in breaking flame stability.

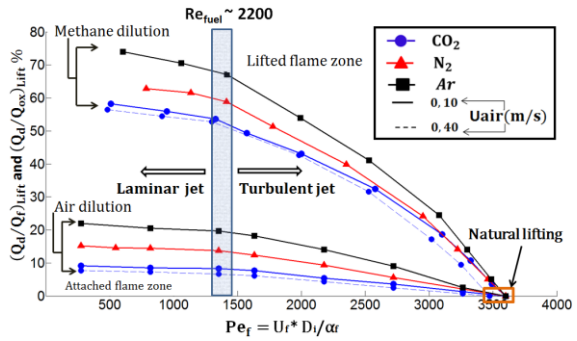

Figure 5. Critical lifting ratios vs. Pe_f for both sides dilution

The flame sensitivity to lift off the flame has been characterized by the critical ratios measured at lifting, $(Q_d/Q_{ox})_{lift}$ and $(Q_d/Q_f)_{lift}$. Q_d, $Q_f = Q_{CH4} + Q_d$ and $Q_{ox} = Q_{air} + Q_d$ are the volumetric flows rates of the diluent, fuel and oxidant respectively. A map of the attached flame stability is established in the 2D physical domain (Pe_f , Q_d/Q_{ox} or Q_d/Q_f) under given U_{air}. Fig. 5 presents curves for two air velocities, described by the relationships at the flame lift-off $[Pe_f, (Q_d/Q_{ox})_{lift}]=0$ for the **air-dilution** and $[Pe_f, (Q_d/Q_f)_{lift}]=0$ for the **methane-dilution** configurations. Pe_f is the Peclet number calculated with the fuel (CH_4+diluent) properties in the final mixing when lift-off occurs: $Pe_f = (U_{f\text{-}lift}*D_i) /\alpha_{f\text{-}lift}$ with $\alpha_{f\text{-}lift}$ the thermal diffusivity. In the air dilution the quantities remains those of the pure methane. Pe_f describes the balance between inertia and thermal diffusivity phenomena. Increasing U_{air} from 0.1 to 0.4 m/s shifts the curves to lower values by keeping the same variation-type as dilution is performed in the air stream as well as in the methane stream (see fig. 5). The curves have negligible sensitivity to the air velocity in that range of values. In the following U_{air} =0.1 m/s is chosen to illustrate results. The analysis is valid whatever U_{air}. The curves in fig. 5 are dependent on: i) the aerodynamic and thermal diffusivity conditions characterized by Pe_f, ii) the nature of the diluent. All the profiles systematically decrease when Pe_f increases: a slow decrease of diluents amount for $Pe_f < 1500$, then a steeper one until reaching the natural lift-off by aerodynamics only. The modification in the slopes occurs at $Re_f \sim 2200$ resulting from the change in the jet behavior from the laminar to the turbulent regime. The diluent capability to break the anchored flame stability from the strongest to the weakest one evolves in the same manner for both sides dilution configuration. CO_2 has the strongest ability, followed by N2 and finally by Ar, such that: $(Q_{CO2})_{lift} < (Q_{N2})_{lift} < (Q_{Ar})_{lift}$.

Describing lifting limits leads to two self-similarity laws whatever the diluents, one for the methane dilution and the other for the air dilution. They are reported in table 1. K_d is a comparative parameter characterizing the capability of a diluent to break the flame stability relative to that of CO_2, $K_{d,i} = (Q_d/Q_i)_{lift}/(Q_{CO2}/Q_i)_{lift}$ with i=ox or f in the air and methane side dilution respectively. K_d does not vary with U_{air} conditions. The search of limits with other chemically weak diluents can be deduced from those of CO_2 once K_d known.

a. **Methane-dilution** $(Q_d/Q_f)_{lift}/K_{d,f} = \delta Pe_f^2 + \lambda Pe_f + \kappa$

δ	-6 * 10-6
λ	5 * 10-3
κ	56.6

Diluent	$K_{d,f}$
CO2	1
N2	1.13
Ar	1.28

b. **Air-dilution** $(Q_d/Q_{ox})_{lift}/K_{d,ox} = \alpha 1(\alpha 2)Pe_f + \beta 1(\beta 2)$

Regime	α1, β1 $Re_{CH4} \le 2200$	α2, β2 $Re_{CH4} > 2200$
α (10-4)	9	4.2
β (10-4)	10	15

Diluent	$K_{d,ox}$
CO2	1
N2	1.69
Ar	2.46

Table 1. Coefficients defining lifting limit for both sides dilution

Comparing dilution in the two sides shows that $(Q_d/Q_f)_{lift}$ is 3 to 6 times higher than $(Q_d/Q_{ox})_{lift}$ depending on the chosen diluent. This large difference is interpreted by a flame leading-edge approach in sec. 3.3.

3.3. Flame-leading-edge approach

The leading-edge or reaction kernel was described in the work of Takahashi et al. [3] as the highest spot with a heat release rate peak formed in a partially premixed region at the flame base. It provided a continuous ignition source sustaining the stable combustion by holding the trailing diffusion flame in the flow for supporting the flame. Min et al. [1,2] investigated the influence of the air dilution (CO_2, N_2, and Ar) on the flame lifting. They found that the air/methane premixed flame propagation velocity S_l calculated with the diluent amounts at lifting appeared to be the same for the three diluents. They suggested that stabilization at the flame base in which the gases CH_4, air and diluent were assumed premixed was mainly piloted by the flame-leading-edge mechanism, ensuring a balance between S_l and the incoming gases velocity. Here, the approach is extended for methane dilution too. The air/CH_4 reaction at stoichiometry follows the global one-step equation:

$$1CH_4 + 2(O_2 + 3.76N_2) + N_{d,lift}D \rightarrow CO_2 + 2H_2O + 7.52N_2 + N_{d,lift}D \qquad 1$$

$N_{d,lift}$ is the moles of the diluent D added to the CH_4 or to the air when the flame is nearby lifting such as $N_{d,f-lift} = (Q_d/Q_{CH4})_{lift}$ and $N_{d,ox-lift} = 9.52 \times (Q_d/Q_{air})_{lift}$. Therefore, lifting can be characterized by the critical molar fraction X^d_{lift} at the leading-edge on the basis of the critical flow rate ratios as follows:

$$X^d_{f-lift} = \left(1 + 10.52\left(\frac{Q_{CH4}}{Q_d}\right)\right)^{-1}, X^d_{ox-lift} = \left(1 + 1.1\left(\frac{Q_{air}}{Q_d}\right)_{lift}\right)^{-1} \qquad 2$$

Fig. 6 presents X^d_{f-lift} and $X^d_{ox-lift}$ as functions of Pe_f

for the 3 diluents. It is remarkable that for a given diluent the two critical molar fractions at lifting: $X^d_{ox-lift} \sim X^d_{f-lift}$, are very similar, the large difference observed in Fig. 5 between $(Q_d/Q_{ox})_{lift}$ and $(Q_d/Q_f)_{lift}$ being no more observed. It suggests that leading-edge drives flame lifting at the main order. However, small discrepancies persist for a given Pe_f value. To explain that, $X^d_{ox-lift}$ - X^d_{f-lift} is plotted in fig.7 as a function of the initial velocity U_{CH4}. The difference between X^d_{f-lift} and $X^d_{ox-lift}$ for a given U_{CH4} increases as experiments are carried out with CO_2, then N_2, and finally Ar.

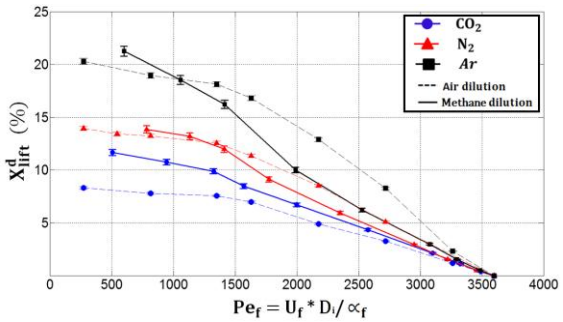

Figure 6. $X^d_{ox-lift}$ and X^d_{f-lift} as a function of Pe_f at U_{air}=0.1 m/s.

It evolves in the same manner as that is noted for the induced mechanical impacts exposed in sec. 3.1. In particular, for a given diluent, $X^d_{ox-lift}$ - X^d_{f-lift} like the mechanical impact, is maximum at $U_{CH4} \sim 5.5$ m/s, marking the change in the methane jet regime from laminar to turbulent (Re_{CH4} ~2200).

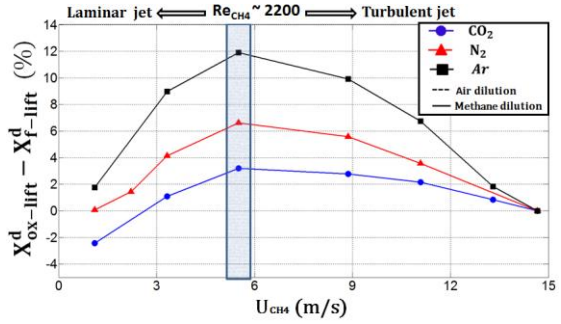

Figure 7. $X^d_{ox-lift}$ - X^d_{f-lift} as a function of U_{CH4} at U_{air}=0.1 m/s.

This feature highlights that the difference between molar fractions at lifting reported in fig. 7 results from the existence of the mechanical effects since the latter ones participate in moving the flame in the framework of a semi-thick rim. Influence of the trailing diffusion flame [3] or differential diffusion mechanisms may also impact the flame detachment condition at the second order.

4. Leading-edge location: H_a and Radius R_a

4.1 Attachment flame location: R_a, H_a

As the diluent is added to one of the streams (methane or air), the leading-edge location is followed in the physical space ($R_a/R_a°$, $H_a/H_a°$) parametrized by the diluent molar fraction X^d normalized by its value at lifting X^d_{lift}. Fig. 8 and fig. 9 report data corresponding to the fuel jet initially in the laminar regime (U_{CH4}=1.1 m/s) and in the turbulent regime (U_{CH4}=8.9 m/s) respectively both performed at U_{air}=0.1 m/s. All the curves start from the non-diluted location defined by $H_a/H_a° = 1$ and $R_a/R_a° = 1$. The initial location of the flame-leading-edge above the burner rim and its displacement area are indicated in a sketch beneath each diagram.

Air-side dilution (dot lines) slightly modifies R_a which remains almost constant $R_a / R_a° \sim 1$ whatever the diluent. This quasi unchanged lateral displacement results from some weak aerodynamic modifications performed in the burner vicinity when the diluent is added to the air [1]. In particular, mechanical impacts are negligible as explained in sec. 3.1. Contrary to the radius, flame attachment height $H_a/H_a°$ is strongly modified. Increasing diluent addition in the air side moves up the flame along a vertical path until a height is reached for which the flame can no more stabilize and ultimately lifts off. Adding a diluent in the air stream stabilizes the flame axially farther downstream to the burner rim but at the same radial position.

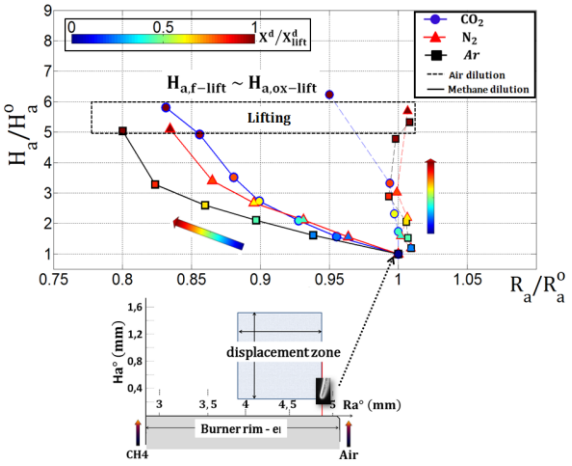

Figure 8. $\frac{H_a}{H_a^\circ}$ vs $\frac{R_a}{R_a^\circ}$ parametrized by X^d/X^d_{lift} at U_{CH4}=1.1 m/s.

On the other hand, dilution in the **methane-side** (solid lines) modifies both $H_a/H_a°$ and $R_a/R_a°$. The flame stabilizes at a new location moving simultaneously downstream to a higher H_a and radially, closer to the fuel jet to a smaller R_a. As the diluent amount is increased, the most abrupt H_a increase is noted for CO_2 followed by N_2, and then Ar. The same value of $H_a/H_a°$ is found with the same X^d/X^d_{lift} whatever the diluents (see color bar).

X^d_{lift} appears as a key element in the flame stabilization involving dilution. In particular, under fixed initial aerodynamic conditions H_a/H_a^o evolves as a unique curve, following exponential relationships fitted by a least square method: $Ha/Ha^o = \exp\left[A_i \; X^d_i / X^d_{i-lift}\right]$, with subscript i equal to ox or f. A_f = 1.65, 1.18 and 0.44 and A_{ox} = 1.59, 1.31 and 0.75 for U_{CH4}=1.1, 2.5 and 8.9 m/s respectively. These curves flatten when the initial velocity U_{CH4} is increased. Aerodynamics competes with dilution for detaching the flame, even though in that physical domain aerodynamics cannot detach the flame by its own action, contrary to dilution.

As shown in fig. 5, the transition of the jet regime from the laminar to the turbulent one influences the behavior of the critical ratios $(Q_d/Q_{ox})_{lift}$ and $(Q_d/Q_f)_{lift}$. The lifting limit slightly depends on the fuel jet modifications provided that the jet regime is still laminar, while it is strongly influenced by those ones when the final regime becomes turbulent. As a consequence, the attachment height adapts its evolution by repeating these features.

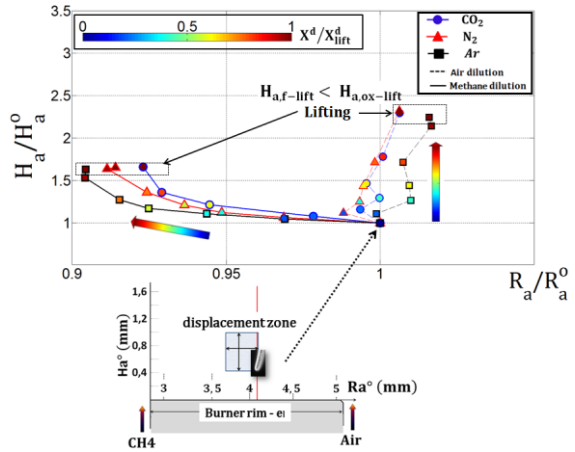

Figure 9. $\frac{H_a}{H_a^\circ}$ vs $\frac{R_a}{R_a^\circ}$ parametrized by X^d/X^d_{lift} at U_{CH4}=8.9 m/s.

Examples are reported in Figs. 8 and 9. For U_{CH4}=1.1 m/s (Re_{CH4} ~ 420), $H_{a,lift}$ measured in the two diluted configurations is nearly constant: $H_{a,ox\text{-}lift}$ ~ $H_{a,f\text{-}lift}$ (Fig. 8). It relies on the fact that the fuel stream regime is unchanged. Indeed, the fuel stream initially laminar remains laminar even when lifting is achieved further to dilution in the methane side for which the fuel velocity U_f varies from 2.5 to 3.7 m/s (Re_f ~ 1595 and 1745) according to the diluent. The flame lifts off at the same value of $H_{a,lift}$ whatever the side where dilution is performed. On the contrary, at U_{CH4}=8.9 m/s (Re_{CH4} ~ 3345) the jet is already turbulent; when methane is diluted turbulence is enhanced, while with dilution in the air-side, turbulence is unchanged. So, air-diluted flames lift off at a higher location than the methane diluted flames: $H_{a,ox\text{-}lift} > H_{a,f\text{-}lift}$ (see fig. 9). The difference $H_{a,ox\text{-}lift} - H_{a,f\text{-}lift}$ is also maximum at R_{CH4} ~2200.

4.2 R_a/R_a^o controlled by impulsion

For a given initial methane jet velocity, R_a remains constant even though a diluent is added to the air flow.

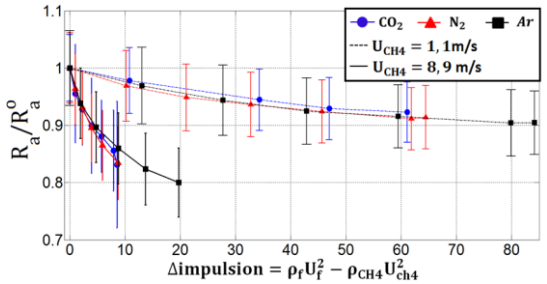

Figure 10. Ra/Ra° vs Δimpulse at U_{air}=0.1 m/s. Methane dilution

By contrast, it decreases as the diluent is added into the fuel. Data R_a/R_a^o are plotted in fig. 10 against the fuel jet impulse variation. They follow the same curve whatever the diluents, indicating that R_a is controlled by the differential fuel jet momentum flux between the initial and current dilution states.

5.0 Concluding remarks

Flame lifting has been studied for attached non-premixed flames where the air co-flow or methane jet are diluted by CO_2, N_2 or Ar. The analysis is carried out for jet velocities covering the hysteresis flame-stability domain in which flames can be attached or lifted.

Lifting limits are experimentally determined by the critical ratios $(Q_d/Q_i)_{lift}$ with *i* = "ox" or "f" according to whether dilution is made in the air or methane side. By introducing a comparative parameter $\mathbf{K_{d,i}}$ characterizing the ability of a diluent to break flame stability relative to that of CO_2, self-similarity relationships at lifting, satisfied whatever the diluents, have been expressed such that $(Q_d/Q_i)_{lift}/K_{d,i}$ are functions of Pe_f. Pe_f is the Peclet number which takes into account both inertia and thermal diffusivity effects of the fuel (diluted) jet. The knowing of the limit for CO2 and of $K_{d,i}$ is then sufficient to deduce the limits resulting from the dilution of reactant *i*. The diluent percent used to detach the flame with methane dilution are much higher than those in air dilution. The large difference $(Q_d/Q_{ox})_{lift}$ - $(Q_d/Q_f)_{lift}$ is interpreted by a flame-leading-edge approach where the gases CH_4, air and diluent are assumed premixed at the flame base. Stabilization is then ensured by a balance between the incoming gas velocity and S_l.

The leading-edge location is marked by the attachment height H_a and radius R_a. H_a-changes are driven at the main order by dilution. H_a evolves as a unique law for a given diluted side configuration, dictated by the affine parameter X^d/X^d_{lift} whatever the diluents. On the contrary R_a-changes are piloted at the main order by fuel-jet momentum-flux increases further to dilution. R_a follows self-similarity relationships expressed with the impulse variation $\rho_f U_f^2 - \rho_{CH4} U_{CH4}^2$. The behavior response of the system shows that the investigation can focus on CO_2, since H_a and R_a obtained with other diluents can be deduced from those defined by CO_2 via the self-similarity laws found here.

References

[1] J. Min, F. Baillot, A. Wyzgolik, E. Domingues, M. Talbaut, B. Patte-Rouland, C. Galizzi, Combust. Sci. Technol. 182(2010): 1782-1804

[2] H. Guo, J. Min, C. Galizzi, D. Escudié, F. Baillot Combust. Sci. Technol. 182(2010): 1549-1563

[3] F. Takahashi, G. Linteris, V. Katta Proc. Combust. Inst. 31(2007) 2721-2729

[4] A. Wyzgolik, F. Baillot, Proc. Combust. Inst. 31(2007): 1583-1590

[5] M. Juniper, S. Candel, J. Propuls Power. 19 (2003)332

[6] Y. Otakayema, T. Tokomori, M. Mizomoto, Proc. Combust Inst. 32(2009): 1091-1097

[7] A. Lock, A. Briones, S. Aggarwal, I. Puri and U. Hegde, Combust. Flame, 149 (2007): 340-352.